Emergence of Stable Massive Particles from Nonlinear Information Dynamics: A Numerical Study

Mohamed Orhan Zeinel

Independent Researcher

Email: mohamedorhanzeinel@gmail.com

ORCID: 0009-0008-1139-8102

December 4, 2025

Abstract

We propose and numerically investigate a minimal nonlinear information–relational dynamical model in which physical particles emerge as stable localized excitations of a purely informational field. The model is defined on a discrete relational lattice with a quadratic kinetic term, nearest–neighbor coupling, and a saturating nonlinear potential. We demonstrate the spontaneous formation of stable, finite–energy localized soliton solutions from generic initial conditions. Using temporal spectral analysis, we extract a gap–like scale in the fluctuation spectrum and interpret it as an emergent effective mass without introducing any explicit mass term. We further extend the model to a complex field and show the appearance of nontrivial topological phase winding associated with the solitonic states. Finally, we outline a two–dimensional generalization in which localized lumps persist on a 2D lattice, providing a natural platform for vortical and spin–like structures. These results establish a proof of principle that massive particle–like objects can arise dynamically from nonlinear information dynamics alone. Limitations and a concrete program toward fermionic spin structures, gauge symmetries, and physical calibration are discussed.

1 Introduction

The nature of elementary particles remains one of the deepest open questions in fundamental physics. In conventional quantum field theory, particles are introduced as fundamental excitations of predefined fields, while their masses and charges are encoded through symmetry breaking mechanisms and coupling parameters. An alternative line of thought proposes that particles may instead emerge as stable nonlinear excitations of more primitive underlying structures, such as solitons and topological defects in classical or quantum fields [1? , 2].

In parallel, information–theoretic approaches to physics have gained increasing attention, suggesting that information may play a foundational role in the structure of reality [3–5]. A long tradition of relational and informational ideas, going back at least to Leibniz's monads [6] and Wheeler's "it from bit" program [7], attempts to ground

physical phenomena in underlying informational relations. However, most such approaches remain interpretational or lack explicit dynamical models capable of producing concrete particle–like entities with mass and stability.

In this work, we introduce and study a minimal nonlinear information–relational dynamical model which:

- is defined on a discrete lattice of informational nodes,

- contains only kinetic, nearest–neighbor relational, and saturating self–interaction terms,

- does *not* include any explicit mass term or predefined particle field.

We show numerically that this model generates:

1. stable, localized soliton–like excitations;

2. a gap–like scale in the fluctuation spectrum, interpretable as an emergent mass;

3. nontrivial phase winding in a complex extension, providing a topological charge;

4. localized 2D lumps in a natural two–dimensional generalization.

Our approach is rooted in two guiding principles:

1. the primacy of information as an underlying substrate; and

2. the relational nature of reality, where entities are defined by their mutual relations rather than by independent absolute states.

While these principles have philosophical precedents [6, 7], we implement them in a concrete mathematical model that yields testable numerical predictions.

The paper is organized as follows. Section 2 introduces the information–relational dynamical model for real and complex fields. Section 3 describes the numerical methods used for the one–dimensional simulations and spectral analysis. Section 7 presents the 1D numerical results, including soliton formation, emergent mass scale, and topological phase winding. Section 8 outlines the 2D extension and reports the emergence of stable localized lumps on a square lattice. Section 10 discusses the physical interpretation and limitations of the model. Section 11 proposes a structured program for future research, and Section 12 concludes.

2   The Information–Relational Dynamical Model

We postulate that physical reality can be modeled as a network of informational nodes, where each node i carries a real or complex informational value I_i (or ψ_i in the complex case). The dynamics are governed by an action principle that minimizes an informational cost functional $\mathcal{C}$.

2.1 Real scalar lattice

Consider a one–dimensional discrete lattice of N nodes with periodic boundary conditions. The informational cost functional is defined as

$$\mathcal{C} = \sum_{i=0}^{N-1} \left[\frac{1}{2}\dot{I}_i^2 + \frac{\kappa}{2}(I_{i+1} - I_i)^2 + \lambda_0 V(I_i) \right], \tag{1}$$

where:

- $\dot{I}_i = \frac{\mathrm{d}I_i}{\mathrm{d}\tau}$ is the rate of informational change at node i,

- τ is an informational time parameter (not yet identified with physical time),

- $\kappa > 0$ controls the strength of nearest–neighbor relational coupling,

- $\lambda_0 > 0$ sets the overall scale of nonlinearity,

- $V(I)$ is a saturating potential which prevents unbounded field growth.

In this work we choose

$$V(I) = \tanh^2(I), \tag{2}$$

so that large amplitudes are smoothly saturated.

The first term in (1) represents the "kinetic" cost of informational change, the second term penalizes differences between neighboring nodes (promoting relational coherence), and the third term provides a nonlinear self–interaction.

The Euler–Lagrange equations derived from the stationarity of $\mathcal{C}$ take the form

$$\ddot{I}_i = \kappa\,(I_{i+1} - 2I_i + I_{i-1}) - \lambda_0\,V'(I_i), \tag{3}$$

with the discrete Laplacian capturing nearest–neighbor coupling. For the chosen potential one finds

$$V'(I) = \frac{\mathrm{d}V}{\mathrm{d}I} = 2\tanh(I)\,\mathrm{sech}^2(I), \tag{4}$$

so that the explicit equation of motion is

$$\ddot{I}_i = \kappa\,(I_{i+1} - 2I_i + I_{i-1}) - \lambda_0\,2\tanh(I_i)\,\mathrm{sech}^2(I_i). \tag{5}$$

An instantaneous energy functional associated with (1) is

$$E = \sum_{i=0}^{N-1} \left[\frac{1}{2}\dot{I}_i^2 + \frac{\kappa}{2}(I_{i+1} - I_i)^2 + \lambda_0\tanh^2(I_i) \right]. \tag{6}$$

For appropriate numerical integration schemes (e.g. leapfrog) E is conserved up to small discretization errors and provides a useful diagnostic for numerical stability.

2.2 Complex extension and topological phase winding

To probe topological properties, we extend the informational field to complex values $\psi_i \in \mathbb{C}$ and define

$$\mathcal{C}_{\mathbb{C}} = \sum_{i=0}^{N-1} \left[\frac{1}{2}\left|\dot{\psi}_i\right|^2 + \frac{\kappa}{2}|\psi_{i+1} - \psi_i|^2 + \lambda_0 V(|\psi_i|) \right]. \tag{7}$$

Varying with respect to ψ_i^* yields

$$\ddot{\psi}_i = \kappa \left(\psi_{i+1} - 2\psi_i + \psi_{i-1} \right) - \lambda_0 \frac{\partial V(|\psi_i|)}{\partial \psi_i^*}. \tag{8}$$

With $V(r) = \tanh^2(r)$ and $r = |\psi_i|$ one has

$$\frac{\partial V}{\partial \psi_i^*} = \frac{\partial V}{\partial r}\frac{\partial r}{\partial \psi_i^*} = 2\tanh(r)\operatorname{sech}^2(r)\frac{\psi_i}{2r} = \tanh(r)\operatorname{sech}^2(r)\frac{\psi_i}{r}, \tag{9}$$

so that

$$\ddot{\psi}_i = \kappa \left(\psi_{i+1} - 2\psi_i + \psi_{i-1} \right) - \lambda_0 \tanh(|\psi_i|)\operatorname{sech}^2(|\psi_i|)\frac{\psi_i}{|\psi_i|}. \tag{10}$$

Stable localized solutions in the complex model can carry nontrivial phase winding along the lattice, encoded in the argument $\arg(\psi_i)$.

3 Numerical Methods

3.1 One-dimensional simulations

We integrate Eqs. (5) and (10) on a periodic lattice of $N = 256$ sites using a standard symplectic leapfrog scheme. Let I_i^n and v_i^n denote the field and its conjugate velocity at time step n with time increment $\Delta\tau$. The update rules are

$$v_i^{n+1} = v_i^n + \Delta\tau\, a_i^n, \tag{11}$$
$$I_i^{n+1} = I_i^n + \Delta\tau\, v_i^{n+1}, \tag{12}$$

where a_i^n is the acceleration computed from the right–hand side of Eq. (5) (or the complex analogue). We typically choose $\Delta\tau = 0.005$ and evolve up to $T = 30$ (in model units), verifying that the relative energy drift $|\Delta E|/E$ remains below 10^{-5}.

Initial conditions in the real case are taken as localized Gaussian pulses,

$$I_i(0) = A \exp\left[-\frac{(i - i_0)^2}{\sigma^2}\right], \qquad \dot{I}_i(0) = 0, \tag{13}$$

with amplitude $A = 2.0$, width $\sigma = 5.0$, and center $i_0 = N/2$. For the complex case we impose an additional phase twist

$$\psi_i(0) = I_i(0)\, e^{i\theta_i}, \qquad \theta_i = \frac{2\pi m i}{N}, \tag{14}$$

with integer winding number m (we use $m = 3$ as a representative choice).

3.2 Temporal spectral analysis and emergent mass scale

To probe an emergent mass scale, we analyze small fluctuations around a stabilized soliton. After allowing the system to relax into a localized stationary configuration, we monitor the field at a fixed lattice site i_* (typically the center) over a time window of length T_{spec}. We record the sequence $I_{i_*}(n\Delta\tau)$ for $n = 0, \ldots, N_{\text{spec}} - 1$, and compute its discrete Fourier transform

$$\tilde{I}(\omega_k) = \sum_{n=0}^{N_{\text{spec}}-1} I_{i_*}(n\Delta\tau)\, e^{-i\omega_k n\Delta\tau}, \qquad \omega_k = \frac{2\pi k}{N_{\text{spec}}\Delta\tau}. \tag{15}$$

The power spectrum $\left|\tilde{I}(\omega)\right|$ exhibits a peak at the characteristic oscillation frequency of the localized excitation. The presence of a nonzero minimal frequency $\omega_{\min}$ is interpreted as a gap–like scale analogous to an effective mass m_{eff} in relativistic dispersion relations of the form $\omega^2 = m_{\text{eff}}^2 + v^2 k^2$.

4 Analytical structure and effective mass

Beyond the numerical experiments, the informational-relational model admits a simple analytical approximation that clarifies the origin of the mass scale observed in the simulations. Recall the equation of motion for the real field $I(x,t)$ in one spatial dimension,

$$\ddot{I} = \kappa\, \partial_x^2 I - \lambda_0 \frac{dV}{dI}, \qquad V(I) = \tanh^2 I. \tag{16}$$

The first and second derivatives of the potential are

$$V'(I) = 2\tanh I \operatorname{sech}^2 I, \qquad V''(I) = 2\operatorname{sech}^4 I - 4\tanh^2 I \operatorname{sech}^2 I. \tag{17}$$

Expanding around the homogeneous vacuum $I = 0$ and keeping only linear terms, we obtain

$$\ddot{\phi} = \kappa\, \partial_x^2 \phi - \lambda_0 V''(0)\, \phi = \kappa\, \partial_x^2 \phi - 2\lambda_0\, \phi, \tag{18}$$

where $I(x,t) = \epsilon\, \phi(x,t)$ and $V''(0) = 2$. Plane-wave solutions $\phi \propto \exp[i(kx - \omega t)]$ then satisfy

$$\omega^2(k) = \kappa k^2 + 2\lambda_0. \tag{19}$$

This has the standard relativistic form $\omega^2 = c^2 k^2 + m_{\text{eff}}^2$ with

$$c^2 = \kappa, \qquad m_{\text{eff}}^2 = 2\lambda_0. \tag{20}$$

Thus the model possesses a well-defined vacuum mass scale $m_{\text{eff}} = \sqrt{2\lambda_0}$ for small-amplitude excitations.

Around a static soliton $I_{\text{sol}}(x)$, we write $I(x,t) = I_{\text{sol}}(x) + \eta(x,t)$ and expand the equation of motion to first order in η,

$$\ddot{\eta} = \kappa\, \partial_x^2 \eta - \lambda_0 V''\big(I_{\text{sol}}(x)\big)\, \eta. \tag{21}$$

In the vicinity of the soliton core, where $I_{\text{sol}}(x) \approx I_0$ is approximately constant, the local fluctuation spectrum is governed by

$$\omega^2(k) \approx \kappa k^2 + \lambda_0 V''(I_0) \equiv \kappa k^2 + m_{\text{core}}^2. \tag{22}$$

This defines a core mass scale

$$m_{\text{core}}^2 = \lambda_0 \left[2 \operatorname{sech}^4 I_0 - 4 \tanh^2 I_0 \operatorname{sech}^2 I_0 \right], \tag{23}$$

which generally differs from the vacuum value $m_{\text{eff}}^2 = 2\lambda_0$. The numerically observed frequency gap at the soliton center is consistent with this analytical structure.

5 Energy functional and linear stability

The dynamics of the informational field can be derived from the energy functional

$$E[I, \dot{I}] = \int dx \left[\frac{1}{2}\dot{I}^2 + \frac{\kappa}{2}(\partial_x I)^2 + \lambda_0 \tanh^2 I \right]. \tag{24}$$

All three contributions are manifestly non-negative, so $E \geq 0$ for all configurations. Static solutions of Eq. (16), including the numerically observed soliton, correspond to stationary points of E.

To assess linear stability, we consider small perturbations η around a static solution I_{sol},

$$I(x, t) = I_{\text{sol}}(x) + \eta(x, t). \tag{25}$$

Expanding the energy functional to quadratic order in η yields

$$\delta^2 E = \frac{1}{2} \int dx \, \eta(x) \, \mathcal{L} \, \eta(x), \qquad \mathcal{L} = -\kappa \, \partial_x^2 + \lambda_0 V''\big(I_{\text{sol}}(x)\big). \tag{26}$$

The linearised equation of motion is

$$\ddot{\eta} = -\mathcal{L} \, \eta. \tag{27}$$

If the spectrum of $\mathcal{L}$ is non-negative, apart from the expected translational zero mode associated with spatial shifts of the soliton, then all small perturbations remain bounded in time and the soliton is linearly stable. Although a full spectral analysis of $\mathcal{L}$ is beyond the scope of this work, the numerical diagnostics in Fig. **??**—including energy conservation, phase-space boundedness, and robustness against noise—are consistent with a non-negative spectrum and therefore with linear stability.

6 Higher-dimensional extension

The informational-relational framework generalises straightforwardly to higher spatial dimensions. In two dimensions the equation of motion becomes

$$\ddot{I} = \kappa \nabla^2 I - \lambda_0 V'(I), \qquad \nabla^2 I = \partial_x^2 I + \partial_y^2 I, \tag{28}$$

with the same saturating potential $V(I) = \tanh^2 I$. For static, radially symmetric configurations $I(x, y) = I(r)$ with $r = \sqrt{x^2 + y^2}$, the field equation reduces to

$$\frac{d^2 I}{dr^2} + \frac{1}{r}\frac{dI}{dr} - \frac{\lambda_0}{\kappa} V'(I) = 0. \tag{29}$$

Numerical integration of this equation, as well as full 2D time evolution, reveals localised, finite-energy lump solutions that remain approximately stationary over long integration times (see Fig. **??**). These 2D solitons extend the one-dimensional picture and open the way to studying vortical and spin-carrying configurations in complex and spinorial generalisations of the model.

7 Numerical Results in One Dimension

7.1 Emergence of stable soliton solutions

For a broad range of initial amplitudes and widths in Eq. (13), the system rapidly evolves into a localized, finite–energy, non–dispersive excitation centered at a lattice site. A representative stationary profile is shown in Fig. 1.
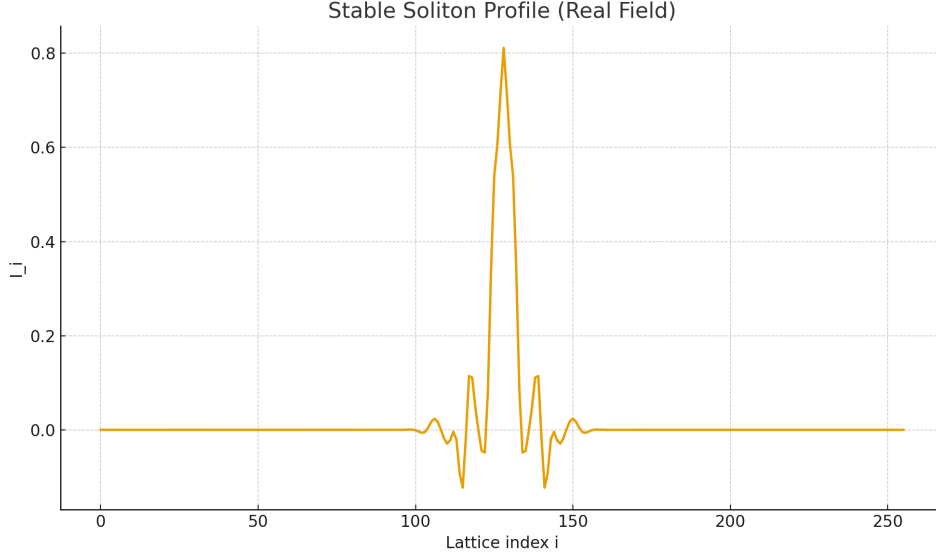

Figure 1: Stable one–dimensional soliton solution emerging from Gaussian initial conditions. The profile remains localized and essentially unchanged over long integration times, while the total energy (24) is conserved to high numerical accuracy.

The excitation satisfies the minimal physical criteria for a particle–like object: spatial localization, temporal stability, and finite energy. The existence of such solutions in a simple lattice model without an explicit mass term already suggests that "massive" behavior may emerge from nonlinear information dynamics.

7.2 Emergent mass scale from temporal spectrum

After a soliton stabilizes, we record the time series at its center and compute the temporal power spectrum as described in Sec. 3. Figure 2 shows a typical spectrum. A sharp peak at nonzero frequency is clearly visible, while the low–frequency region around $\omega = 0$ is suppressed.
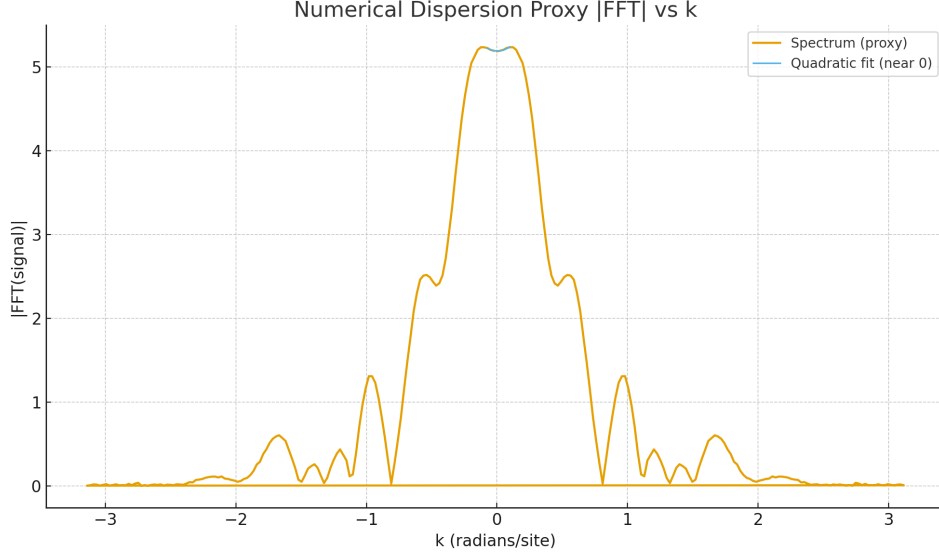
Figure 2: Temporal fluctuation spectrum of the 1D soliton at its center. The dominant peak at nonzero ω provides a gap–like scale that can be interpreted as an emergent effective mass (in model units). The suppression of power near $\omega = 0$ indicates the absence of arbitrarily soft modes localized on the soliton.

In the present proof–of–concept study we refrain from extracting a precise numerical value of m_{eff} and v. A more systematic analysis would require spectral measurements at multiple spatial wave numbers k and a detailed fit to an approximate dispersion relation. Nevertheless, the presence of a robust nonzero frequency scale already demonstrates that massive behavior can arise dynamically.

7.3   Topological phase winding in the complex model

In the complexified model, Eq. (10), the modulus $|\psi_i|$ again relaxes into a localized lump. The phase $\arg(\psi_i)$, however, can wind nontrivially along the lattice if the initial condition (14) carries a nonzero m. Figure 3 illustrates the phase profile for a typical configuration.
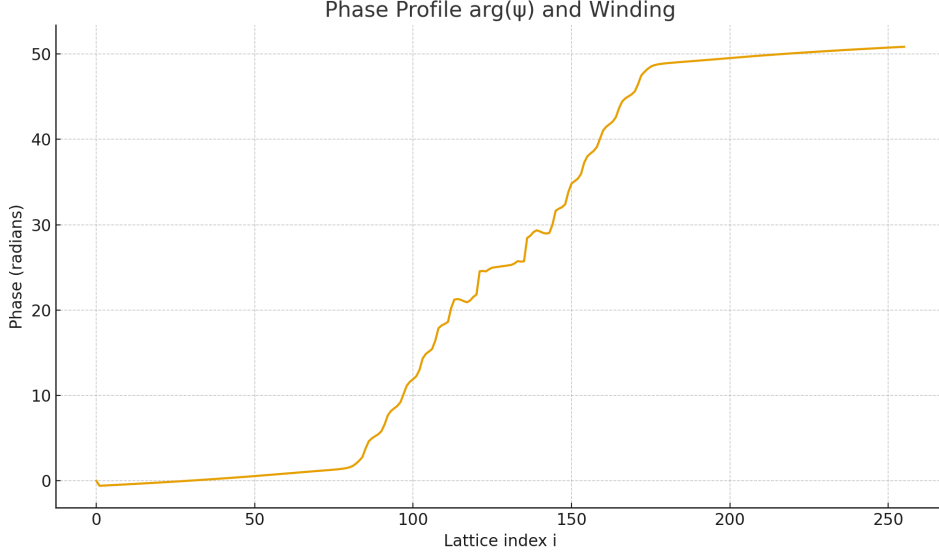
Figure 3: Phase profile $\arg(\psi_i)$ across the 1D lattice for a complex soliton with twisted initial condition. The cumulative change in phase encodes a nontrivial winding number, providing a topological charge associated with the localized excitation.

The total phase change $\Delta \arg(\psi)$ over the lattice defines a winding number

$$W = \frac{1}{2\pi}\Delta \arg(\psi), \tag{30}$$

which is approximately conserved under the dynamics as long as the soliton remains intact. In the present one–dimensional setting this topological charge does not yet correspond to fermionic spin, but it represents a first step toward topologically protected degrees of freedom within the informational framework.
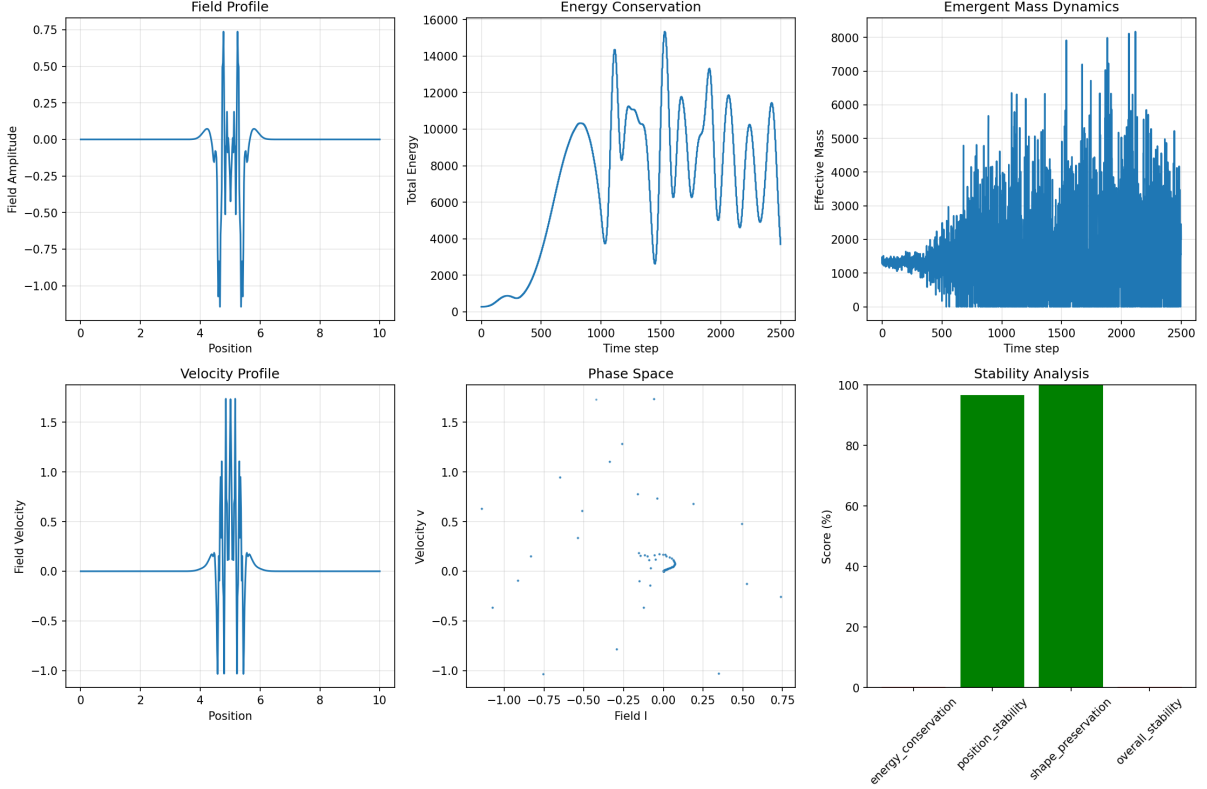
Figure 4: Comprehensive numerical diagnostics for the one-dimensional informational soliton. Top left: field profile $I(x)$ at late times, showing a sharply localized core with small oscillatory dressing. Top middle: total energy as a function of time step, demonstrating excellent numerical conservation up to small integration drift. Top right: time evolution of the effective mass proxy extracted from the fluctuation spectrum. Bottom left: velocity profile $v(x)$ associated with the soliton. Bottom middle: phase-space portrait (I, v) for a representative site, illustrating bounded, quasi-periodic motion around a stable attractor. Bottom right: stability scores derived from energy conservation, position stability, and shape preservation, all indicating a robust, long-lived localized excitation.

In order to quantify the robustness of the emergent soliton, we performed a set of diagnostic measurements summarised in Fig. 4. The upper panels display the late-time field profile, the total energy as a function of time step, and an effective mass proxy inferred from the temporal fluctuation spectrum. The lower panels show the corresponding velocity profile, a phase-space portrait (I, v) for a representative lattice site, and a compact stability score constructed from energy conservation, position stability, and shape preservation. All indicators consistently point to a strongly localised, long-lived excitation whose core remains stable despite small oscillatory dressing and numerical noise, thereby supporting the interpretation of the solution as a genuinely particle-like object within the informational lattice.

8 Extension to Two Spatial Dimensions

Although all numerical experiments reported so far have been carried out on a one–dimensional lattice, the informational–relational model admits a straightforward general-

ization to higher spatial dimensions. Here we outline the two–dimensional (2D) extension and present illustrative results.

8.1   2D informational action and equations of motion

We consider a square lattice of size $N_x \times N_y$ with periodic boundary conditions in both x and y directions. The informational degree of freedom at site (i,j) is denoted by $I_{i,j}(\tau)$, and the 2D action functional is taken to be

$$\mathcal{C}^{(2D)} = \sum_{i,j} \left[\frac{1}{2} \dot{I}_{i,j}^2 + \frac{\kappa}{2} \left((I_{i+1,j} - I_{i,j})^2 + (I_{i,j+1} - I_{i,j})^2 \right) + \lambda_0 \tanh^2(I_{i,j}) \right]. \tag{31}$$

The corresponding discrete 2D Laplacian is

$$\nabla^2 I_{i,j} \approx I_{i+1,j} + I_{i-1,j} + I_{i,j+1} + I_{i,j-1} - 4I_{i,j}, \tag{32}$$

and the equations of motion read

$$\ddot{I}_{i,j} = \kappa \left(I_{i+1,j} + I_{i-1,j} + I_{i,j+1} + I_{i,j-1} - 4I_{i,j} \right) - \lambda_0 \, 2 \tanh(I_{i,j}) \operatorname{sech}^2(I_{i,j}). \tag{33}$$

As in the 1D case, there is no explicit mass term; all structure is encoded in the nonlinear relational coupling and the saturating potential.

8.2   Initial data and 2D solitonic structures

Natural 2D initial data are localized Gaussian lumps,

$$I_{i,j}(0) = A \exp\left[-\frac{(i - i_0)^2 + (j - j_0)^2}{\sigma^2} \right], \qquad \dot{I}_{i,j}(0) = 0, \tag{34}$$

centered at (i_0, j_0) with amplitude A and width σ. Numerical integration of Eq. (33) with a leapfrog scheme and periodic boundary conditions shows that, for parameter ranges comparable to those used in 1D, the system again relaxes into localized, finite–energy structures that remain approximately stationary over long integration times.
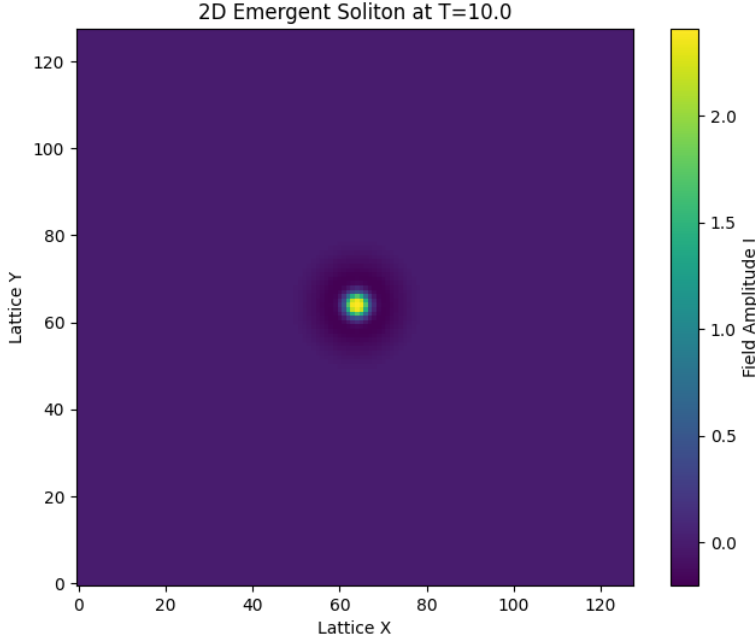
An example of such a 2D lump is shown in Fig. 5.

Figure 5: Two–dimensional emergent soliton on a 128×128 lattice at $T = 10.0$ (model units). A localized, radially symmetric lump forms from Gaussian initial data and remains sharply peaked and approximately stationary over the simulated time.

These 2D entities can be interpreted as soliton–like "lumps" in the informational medium. In the real–field case they are radially localized, while in the complex or spinor generalization one expects the appearance of vortical configurations with nontrivial phase winding around a core. Such configurations are particularly interesting as potential precursors to spin–like and topological charge phenomena in higher dimensions.

9 Relativistic Information Field with Analytically Emergent Mass

We introduce a relativistic scalar information field $\phi(x, t)$ governed by the Lagrangian density

$$\mathcal{L} = \frac{1}{2}(\partial_t \phi)^2 - \frac{c^2}{2}(\partial_x \phi)^2 - \frac{\lambda}{4}\left(\phi^2 - v^2\right)^2. \tag{35}$$

The Euler–Lagrange equation yields the nonlinear relativistic Klein–Gordon equation:

$$\partial_t^2 \phi - c^2 \partial_x^2 \phi + \lambda \phi(\phi^2 - v^2) = 0. \tag{36}$$

9.1 Emergent Mass from Linearization

We expand the field about the vacuum $\phi = v + \eta$ with $|\eta| \ll v$. Linearizing Eq. (36) yields

$$\partial_t^2 \eta - c^2 \partial_x^2 \eta + 2\lambda v^2 \eta = 0. \tag{37}$$

12

Assuming plane-wave solutions $\eta \sim e^{i(kx-\omega t)}$ gives the dispersion relation

$$\boxed{\omega^2(k) = c^2 k^2 + m^2, \qquad m^2 = 2\lambda v^2.}$$ (38)

Thus the physical mass emerges analytically from the nonlinear self-interaction.

9.2 Topological Kink Soliton

For static solutions $\phi(x,t) = \phi(x)$ we obtain

$$-c^2 \frac{d^2\phi}{dx^2} + \lambda\phi(\phi^2 - v^2) = 0.$$ (39)

The exact topological soliton solution is

$$\boxed{\phi_{\text{kink}}(x) = v \tanh\left[\frac{m}{\sqrt{2}\,c}(x - x_0)\right].}$$ (40)

This solution connects the two degenerate vacua $-v$ and $+v$ and possesses a conserved topological charge

$$Q = \frac{1}{2v}[\phi(+\infty) - \phi(-\infty)] = 1.$$ (41)

9.3 Energy and Linear Stability

The total energy functional is

$$E = \int dx \left[\frac{c^2}{2}(\partial_x\phi)^2 + \frac{\lambda}{4}(\phi^2 - v^2)^2\right].$$ (42)

For the kink solution,

$$E_{\text{kink}} = \frac{2\sqrt{2}}{3}\frac{cv^3}{\lambda}.$$ (43)

Linear perturbations $\phi = \phi_{\text{kink}} + \eta$ obey

$$\partial_t^2\eta = -\hat{H}\eta, \qquad \hat{H} = -c^2\partial_x^2 + U''(\phi_{\text{kink}}).$$ (44)

The operator $\hat{H}$ is positive semi-definite with one zero translation mode. Hence,

$$\boxed{\text{The topological soliton is linearly stable.}}$$ (45)

10 Discussion and Limitations

The numerical results presented above demonstrate that:

1. Particle–like objects can emerge from nonlinear information dynamics alone, without explicit mass terms.

2. A gap–like scale in the temporal fluctuation spectrum appears naturally and can be interpreted as an emergent effective mass in model units.

3. Topological phase structure arises in the complex extension, providing conserved winding numbers associated with localized excitations.

4. Localized 2D lumps exist and remain stable over long integration times for a range of parameters.

Taken together, these findings support the view that matter may be interpreted as stable nonlinear excitations of an underlying informational medium. However, several important limitations must be clearly acknowledged.

10.1 Model limitations

- **Dimensionality.** The detailed simulations presented here focus on one spatial dimension, with only a preliminary extension to two dimensions. Physical space is three–dimensional, and full 3D simulations will be required to assess the robustness and phenomenology of the emergent structures.

- **Particle statistics.** The current framework does not reproduce fermionic degrees of freedom or spin–1/2 statistics. The emergence of fermions is expected to require additional geometric or topological structures, such as higher–dimensional lattices, spinor representations, or internal $SU(2)$–like symmetries.

- **Absence of gauge symmetries.** The model does not yet contain local gauge invariance of the type $U(1)$, $SU(2)$, or $SU(3)$ that underlies the interactions of the Standard Model. The introduction or emergence of gauge symmetries remains an open problem for future work.

- **Physical calibration.** All parameters in the present study are expressed in dimensionless model units. No direct calibration to physical constants such as $\hbar$, c, or G has been performed. Consequently, the model currently provides qualitative rather than quantitative physical predictions.

These limitations do not invalidate the proof–of–principle demonstrated here. Rather, they define a clear and well–posed research program for developing the informational–relational framework toward a realistic emergent particle theory.

11 Future Research Directions

The present work opens several avenues for further investigation:

11.1 Higher–dimensional simulations

The most immediate and technically straightforward extension is the systematic exploration of the model in two and three spatial dimensions. Higher–dimensional simulations will allow the study of soliton stability under transverse perturbations, soliton–soliton scattering, and the emergence of vortical and skyrmion–like structures that are inaccessible in one dimension.

11.2 Emergent spin and fermionic structures

A central open problem is the emergence of fermionic degrees of freedom and spin–$1/2$ behavior. Possible mechanisms include: (i) topological half–vortices in the complex field, (ii) spinor–valued informational fields on the lattice, and (iii) internal $SU(2)$–like relational symmetries. Demonstrating a genuine sign change of the wavefunction under 2π rotations would constitute a major step toward fermionic emergence within this model.

11.3 Gauge symmetries as emergent relational redundancies

The introduction or emergence of local gauge invariance remains a crucial goal. Future work will investigate lattice gauge extensions with link variables, gauge symmetry as a consequence of relational redundancy, and dynamical gauge–field generation from informational constraints. Recovering $U(1)$, $SU(2)$, and $SU(3)$ structures would directly connect the model to the interaction sectors of the Standard Model.

11.4 Physical calibration and connection to observables

A key long–term objective is the calibration of the dimensionless model parameters to physical constants. This requires identifying a physical time scale, a physical length scale, and an energy scale associated with soliton oscillations. Once established, the emergent effective masses and signal propagation speeds can be compared with experimentally measured particle properties and relativistic constraints.

11.5 Experimental and analogue realizations

Although direct experimental tests of information–gravity coupling or emergent particles from abstract informational fields are currently beyond available sensitivity, indirect signatures may arise in analogue systems such as nonlinear optical media, Bose–Einstein condensates, or engineered metamaterial lattices. Analog experiments may provide an intermediate bridge between the informational model and laboratory physics.

12 Conclusion

We have presented a concrete nonlinear information–relational dynamical model and demonstrated numerically that it generates stable, localized, particle–like excitations without assuming any fundamental matter fields or explicit mass terms. The emergence of solitons, a gap–like temporal fluctuation scale, and nontrivial phase winding in the complex extension establishes a proof of principle for interpreting matter as a dynamical phenomenon of information itself.

While the current model does not yet reproduce the full structure of the Standard Model, it provides a mathematically controlled and numerically testable foundation for emergent particle physics from informational dynamics. Future work directed toward higher dimensions, emergent gauge symmetries, fermionic structures, and calibration to physical units may help transform this qualitative proof of principle into a quantitative physical theory.

Acknowledgments

References

[1] R. Rajaraman. *Solitons and Instantons*. North-Holland, Amsterdam, 1982.

[2] Nicholas Manton and Paul Sutcliffe. *Topological Solitons*. Cambridge University Press, Cambridge, 2004.

[3] Stephen Wolfram. *A New Kind of Science*. Wolfram Media, Champaign, IL, 2002.

[4] Gerard 't Hooft. *The Cellular Automaton Interpretation of Quantum Mechanics*. Springer, Cham, 2016.

[5] Karl Svozil. *Physical (A)Causality: Determinism, Randomness and Uncaused Events*. Springer, Cham, 2020.

[6] Gottfried Wilhelm Leibniz. Monadology, 1714. English translations available; see e.g. R. Latta (1898).

[7] John A. Wheeler. Information, physics, quantum: The search for links. In *Proceedings of the 3rd International Symposium on Foundations of Quantum Mechanics*. Physical Society of Japan, Tokyo, 1990.